# Scale-Dependent Accuracy in Regional Spectral Methods

HUNG-CHI KUO

*Department of Atmospheric Science, National Taiwan University, Taipei, Taiwan, Republic of China*

R. T. WILLIAMS

*Department of Meteorology, Naval Postgraduate School, Monterey, California*

(Manuscript received 7 August 1997, in final form 1 December 1997)

ABSTRACT

The accuracy of a numerical model is often scale dependent. Large spatial-scale phenomena are expected to be numerically solved with better accuracy, regardless of whether the discretization is spectral, finite difference, or finite element. The purpose of this article is to discuss the scale-dependent accuracy associated with the regional spectral model variables expanded by sine–cosine series. In particular, the scale-dependent accuracy in the Chebyshev-tau, finite difference, and sinusoidal- or polynomial-subtracted sine–cosine expansion methods is considered. With the simplest examples, it is demonstrated that regional spectral models may possess an unusual scale-dependent accuracy. Namely, the numerical accuracy associated with large-spatial-scale phenomena may be worse than the numerical accuracy associated with small-spatial-scale phenomena. This unusual scale-dependent accuracy stems from the higher derivatives of basic-state subtraction functions, which are not periodic. The discontinuity is felt mostly by phenomena with large spatial scale. The derivative discontinuity not only causes the slow convergence of the expanded Fourier series (Gibbs phenomenon) but also results in the unusual scale-dependent numerical accuracy. The unusual scale-dependent accuracy allows large-spatial-scale phenomena in the model perturbation fields to be solved less accurately.

## 1. Introduction

Spectral methods seek the solution to a differential equation in terms of a series of known, smooth functions. The basis functions are often chosen from the eigenfunctions of a Sturm–Liouville problem for the reason of orthogonality and completeness. With the advent of the fast Fourier transform (FFT) and the spectral transform method (Orszag 1970), the spectral method has become a popular choice in atmospheric modeling. It is accurate with the ''exponential convergence'' property. It avoids aliasing error and the pole problem in the global spherical domain. The spectral method conserves the quadratic quantities and is well-suited for climate modeling. Most of all, the spectral method allows the efficient incorporation of the semi-implicit method in global models. The semi-implicit method is important because it allows the time step to be limited mainly by the magnitude of the wind associated with advection. It removes the stability constraint imposed by the fast gravity or acoustic waves. On the other hand, the semi-Lagrangian method removes the stability constraint imposed by the advective process. With the semi-implicit scheme and the semi-Lagrangian method, the time step in an atmospheric model is limited by the accuracy requirement rather than by the stability requirement. The longer time step used in the semi-implicit method allows the physical parameterization package (with the exception of radiation) to be called every time step. With the above advantages, despite the lack of a fast Legendre transform, almost all the operational global models and GCMs are based on the spectral method with spherical harmonic basis functions.

Despite the popularity of global spectral models, there are obstacles for regional spectral models. The obstacles lie in the time-dependent lateral boundary conditions and the implementation of semi-implicit methods. Tatsumi (1986) developed a sinusoidal-subtracted Fourier sine–cosine series expansion method for limited-area modeling. His method in principle is similar to the polynomial-subtracted Fourier sine–cosine series expansion, which is discussed by Gottlieb and Orszag (1977). The method was successfully applied to the operational forecast model at the Japan Meteorological Agency (Segami et al. 1989). Several similar Tatsumi-type spectral methods have also been developed in other places. For example, Machenhauer (1986) and Haugen and Machenhauer (1993) employed the Fourier series in the High-Resolution Limited-Area Model (HIRLAM), Hoyer (1987) used the sine–cosine series in the European Cen-

*Corresponding author address:* Dr. R. T. Williams, Department of Meteorology, Naval Postgraduate School, Monterey, CA 93943-5000. E-mail: williart@met.nps.navy.mil

tre for Medium-Range Weather Forecasts spectral limited-area model (Hoyer-type method hereafter), and Chen and Kuo (1992) used a harmonic-sine series expansion for the partition and reconstruction of limited-area model variables. Juang and Kanamitsu (1994) developed a nested regional spectral method, which consists of a low-resolution global spectral model and a high-resolution sine–cosine-based regional spectral model. More recently, Chen et al. (1997) presented a harmonic-Fourier spectral limited-area model with an external wind lateral boundary condition. Except for differences in the boundary smoothing, these methods differ from each other only in the separation of variables into perturbation and mean. After this separation, the perturbation part of the variable is expanded in Fourier type series for spectral computation. The advantage of Tatsumi-type or Hoyer-type methods lies in the easy incorporation of the semi-implicit method in the regional model. In addition to the semi-implicit method, the Juang and Kanamitsu (Hoyer-type) model allows the regional model to share the same physics and vertical structure with the global spectral model.

Contrary to the Tatsumi-type and Hoyer-type regional methods, Fulton and Schubert (1987a,b) present a summary of the Chebyshev spectral method, including discussions and demonstrations of technique implementation, accuracy, and stability. They also develop a Chebyshev spectral shallow water model in a limited domain, and it yields good results without any boundary smoothing. Kuo and Schubert (1988) have applied the Fourier–Chebyshev method in a Boussinesq nonhydrostatic model to study the evaporative instability of marine boundary layer stratocumulus. Kuo and Williams (1992) discussed the boundary effects in limited-area spectral models. With a simple model, they demonstrated that Tatsumi-type methods do not in general possess the exponential convergence property. The slow convergence of expanded series comes from the fact that the higher derivatives of the expanded function are not continuous at the boundary in a regional model with time-dependent lateral boundary conditions. Thus, the high-resolution calculations of Tatsumi-type methods may not yield high numerical accuracy.

In this article, we discuss the property of scale-dependent accuracy in the regional spectral methods with sine–cosine series. In particular we will show that the perturbation fields in regional spectral models with sine–cosine series expansions may possess an unusual scale-dependent accuracy. Namely, the numerical accuracy of the perturbation fields becomes worse as the spatial scale of the phenomenon gets larger. We will use simple calculations to explore situations in which the derivatives of expanded functions are discontinuous at the time-dependent lateral boundary. Section 2 gives the analysis of the Fourier series and section 3 discusses the model problems and numerical methods. Numerical results without boundary smoothing or filtering are presented in section 4. Section 5 gives concluding remarks.

## 2. Analysis of the Fourier series

Following Lanczos (1956), we will present arguments concerning the effect of boundary conditions on the speed of convergence (accuracy) of the Fourier cosine and sine series. More general analyses of the eigenfunctions of Sturm–Liouville problems can be found in Gottlieb and Orszag (1977) and Fulton and Schubert (1987a).

We consider a function $f(x)$ in the limited domain $[0, \pi]$:

$$f(x) = g(x) + h(x), \tag{2.1}$$

where $g(-x) = g(x)$ is an even function and $h(-x) = -h(x)$ is an odd function.

The $g(x)$ [and the $h(x)$] can then be obtained by the cosine (sine) expansions:

$$g(x) = \frac{1}{2}a_0 + \sum_{k=1}^{\infty} a_k \cos(kx), \tag{2.2a1}$$

$$h(x) = \sum_{k=1}^{\infty} b_k \sin(kx), \tag{2.2b1}$$

with

$$a_k = \frac{2}{\pi}\int_0^{\pi} f(x)\cos(kx)\,dx, \tag{2.2a2}$$

and

$$b_k = \frac{2}{\pi}\int_0^{\pi} f(x)\sin(kx)\,dx. \tag{2.2b2}$$

The speed of convergence can be estimated by the rate at which the spectral coefficient $a_k$ decreases with increasing $k$. The order of the coefficients in the cosine series can be estimated through integration by parts of (2.2a); namely,

$$\frac{2}{\pi}\int_0^{\pi} f(x)\cos(kx)\,dx = -\frac{2}{\pi}\int_0^{\pi} f'(x)\frac{\sin(kx)}{k}\,dx. \tag{2.3}$$

Repeating the process once more,

$$-\frac{2}{\pi}\int_0^{\pi} f'(x)\frac{\sin(kx)}{k}\,dx = \frac{2}{\pi}\frac{f'(x)\cos(kx)}{k^2}\bigg|_0^{\pi} - \frac{2}{\pi}\int_0^{\pi} f''(x)\frac{\cos(kx)}{k^2}\,dx. \tag{2.4}$$

From (2.3) and (2.4) with large $k$, the dominate term for $a_k$ becomes

$$[a_k]_{\text{dom}} = \frac{2}{\pi}\frac{f'(x)\cos(kx)}{k^2}\bigg|_0^{\pi} = \frac{2}{\pi}\frac{(-1)^k f'(\pi) - f'(0)}{k^2}. \tag{2.5}$$

Similar arguments yield the dominate term for the coefficients of the sine series; that is,

$$[b_k]_{\text{dom}} = -\frac{2}{\pi}\frac{f(x)\cos(kx)}{k}\bigg|_0^{\pi} = \frac{2}{\pi}\frac{f(0) - (-1)^k f(\pi)}{k}. \tag{2.6}$$

The integration by parts can be repeated so long as $f(x)$ is sufficiently smooth. If $f(x)$ does not satisfy any specific boundary conditions, then the coefficients of the cosine series decreases at the rate $k^{-2}$, the coefficients of the sine series only at the rate $k^{-1}$.

In Tatsumi-type methods, a sinusoidal function or global model component is introduced as the additional basis to satisfy the time-dependent lateral boundary condition. After subtracting the additional basis from the model variable, the subtracted function or the perturbation part of the variables will then satisfy either of the following homogeneous conditions:

$$f(0) = f(\pi) = 0, \tag{2.7a}$$

$$f'(0) = f'(\pi) = 0. \tag{2.7b}$$

The sine–cosine expansions are then employed for the perturbation variables in the regional spectral method. However, continuity of the higher-order derivatives is not guaranteed in the perturbation variables with time-dependent boundary conditions, regardless of what additional basic mean state is chosen. This discontinuity may occur, for example, when inconsistencies between the regional model and global model develop. Thus, it is expected that the sine series in general converges at the rate of $k^{-3}$, whereas the cosine series converges at the rate of $k^{-4}$, provided that the expanded variable is sufficiently smooth in the limited domain.

This slow convergence in the Fourier series is essentially a reflection of the Gibbs phenomenon associated with the expanded variables not satisfying the periodic condition in the higher-order derivatives. This condition is different from the condition that the higher derivatives be continuous at lateral boundary (which can result from boundary smoothing). The convergence rate depends *only* on the smoothness and on the boundary behavior of the function expanded, regardless how the function is constructed. In the next sections we will use simple calculations to illustrate the impact on the scale-dependent accuracy of the higher derivative discontinuity at the boundary. We will show that the boundary discontinuity not only causes the slow convergence of the expanded Fourier series (Gibbs phenomenon) but also results in an unusual scale-dependent accuracy. The unusual scale-dependent accuracy allows large spatial-scale phenomena in the model perturbation fields to be solved less accurately.

## 3. Model problems

### *a. Advection equation and numerical methods*

The first problem we consider is the one-dimensional linear advection equation:

$$\frac{\partial u}{\partial t} + \frac{\partial u}{\partial x} = 0, \tag{3.1a}$$

in the domain $[-1, 1]$ with the initial condition

$$u(x, t = 0) = \exp\left[-\left(\frac{x + 0.5}{L}\right)^2\right], \tag{3.1b}$$

and the boundary condition

$$u(-1, t) = g(t) = \exp\left[-\left(\frac{-0.5 - t}{L}\right)^2\right]. \tag{3.1c}$$

The analytical solution of this problem is

$$u_{\text{ana}}(x, t) = \exp\left[-\left(\frac{x - t + 0.5}{L}\right)^2\right]. \tag{3.2}$$

This is the simplest model involving wave or advective processes. The incoming boundary condition (3.1c) is specified according to the analytical solution $u_{\text{ana}}(-1, t)$. No boundary condition is needed at $x = 1$. This is an open boundary situation in the sense that any wave should propagate out of the domain without any difficulty. As in Kuo and Williams (1992), we will solve the above problem with polynomial-subtracted (PST), sinusoidal-subtracted (SST) sine series expansion of the Tatsumi-type method, the fourth-order finite-difference method (FD4), and the Chebyshev $\tau$ method. The Gaussian function is used because it is infinitely differentiable. The Gaussian function as well as the analytical boundary condition (3.1c) allow the numerical error to be determined as a function of the spatial-scale parameter (Gaussian $e$-folding distance) $L$.

The $\tau$ and FD4 equations for our model problem (3.1) can be found in Kuo and Williams (1992). Note that the physical points used for a fast discrete Chebyshev transform are $\overline{x}_j = \cos(j\pi/N)$ for $j = 0, \ldots, N$. These points have irregular spacing, which are of $O(1/N^2)$ near the boundary. This irregular grid spacing complicates the time-differencing efficiency in the $\pi$ method. The PST and SST methods can be found in Kuo and Williams (1992). They are the same as illustrated in Gottlieb and Orszag (1977) and Tatsumi (1986). The two methods differ only in the choice of basis functions that satisfy the time-dependent boundary condition. For the *PST* scheme we seek the solution of (3.1) as the sum of a linear polynomial and a sine series:

$$u(x, t) = \frac{\overline{u}(1, t) - g(t)}{2}x + \frac{\overline{u}(1, t) + g(t)}{2} + \sum_{n=1}^{N} \tilde{v}_n(t)\sin\left[n\left(\frac{\pi}{2}x + \frac{\pi}{2}\right)\right], \tag{3.3}$$

where $\overline{u}(1, t)$ in (3.3) is the computed value at $x = 1$ by the PST method. For the SST method, we seek solutions of (3.1) as the sum of a time-dependent sinusoidal function and a sine series. The time-dependent sinusoidal basis is

$$h_{\sin}(x, t) = \frac{\overline{u}(1, t) - g(t)}{2} \sin\left(\frac{\pi}{2}x\right) + \frac{\overline{u}(1, t) + g(t)}{2}. \tag{3.4}$$

These additional time-dependent bases are introduced to satisfy the time-dependent lateral boundary conditions and thus allow the subtracted functions to be expanded in sine series. Note that the subtracted functions may be periodic in their function values at the boundary, but there is no guarantee that they will be periodic in the higher derivatives. Even though the variable separation in our advection test differs greatly from Hoyer-type method, our results should apply equally to the perturbation fields in Hoyer-type method when the perturbation fields do not satisfy the periodic condition in higher derivatives. Our next model problem involves neither the Tatsumi-type nor the Hoyer-type procedure of variable separation.

### *b. Poisson equation and numerical method*

The crucial factor for an efficient atmospheric model lies in the implementation of the semi-implicit method. Similar to the spherical harmonics–based global spectral method, the Tatsumi-type or Hoyer-type method allows the efficient use of the semi-implicit method. With the subtracted variables expanded in terms of Fourier, sine–cosine series, the FFT is used to cut down the computation cost of transformation between spectral and physical space. The solution of the Poisson equation, as required in the semi-implicit method, is of trivial effort in the spectral space when the Fourier type of basis function is employed.

We now consider the two-dimensional Poisson problem:

$$\nabla^2 u = f, \tag{3.5a}$$

in $[-1, 1]$ by $[-1, 1]$ domain with the right-hand side function $f$ defined as

$$f = \exp\left[-\left(\frac{x}{L}\right)^2 - \left(\frac{y}{L}\right)^2\right]\frac{4}{L^4}(x^2 + y^2 - L^2). \tag{3.5b}$$

The $e$-folding distance $L$ again will be used to indicate the spatial scale. With the boundary conditions

$$u(-1, y) = u(1, y) = \exp[-(1 + y^2)/L^2] \qquad -1 \le y \le 1, \tag{3.6a}$$

and

$$u(x, -1) = u(x, 1) = \exp[-(x^2 + 1)/L^2] \qquad -1 \le x \le 1, \tag{3.6b}$$

we have the analytical solution for (3.5) as

$$u(x, y)_{\text{ana}} = \exp\left(-\frac{x^2 + y^2}{L^2}\right), \tag{3.7}$$

in $[-1, 1]$ by $[-1, 1]$ domain. To test the boundary effect on the scale-dependent accuracy, instead of using (3.6) as the boundary condition for (3.5), we will solve (3.5) with the zero boundary condition of $u = 0$. Even though the analytical solution in (3.7) does not show $u = 0$ along the boundary, the boundary condition is purposely set to zero so as to introduce a small error into the boundary condition. The point is then to see how the unusual scale-dependent accuracy results from the small error in the boundary condition. Note that the Poisson equation test here involves neither the Tatsumi-type nor the Hoyer-type procedure of variable separation.

The numerical solution will then be compared with (3.14) to see how the small difference (discontinuity) at the boundary affects the numerical solution. For simplicity, we term the difference between the numerical solution and (3.7) as the error. The spectral method with double Fourier bases and the second-order finite-difference (FD2) with a multigrid technique (Fulton et al. 1986) are used.

## 4. Numerical results

### *a. Advection equation*

The fourth-order Runge–Kutta time integration scheme is used for the time integration for the FD4, $\tau$, PST, and SST methods, with the time step chosen to be very small so that the errors in the computation are dominated by spatial discretization errors.

Figure 1a gives the root-mean-square errors (in log form) in numerical solutions of the model problem (3.1a)–(3.1c) as a function of the spatial-scale parameter $L$ (Gaussian $e$-folding distance) at $t = 1.0$ for $N = 32$. The $\tau$ method clearly gives a much better approximation than does the FD4 method as $L$ increases. In particular, the $\tau$ method reaches machine accuracy $[O(10^{-6})]$ when $L \ge 0.3$. We note that the errors in the SST and PST methods in Fig. 1a are "V" shaped with respect to the spatial size parameter $L$. The minima in these V-shaped curves are associated with $L = 0.2$, a spatial scale that is about one-fifth of the domain in this calculation. On the left part of the V-shaped curves, the error decreases as $L$ increases. This agrees with the FD4 and $\tau$ methods in that the larger spatial-scale phenomena can be computed with a better numerical accuracy. On the right part of the V-shaped curves where $L \ge 0.2$, the numerical accuracy decreases as $L$ increases. Namely, the numerical accuracy associated with larger spatial-scale phenomena is worse than the numerical accuracy associated with smaller spatial-scale phenomena.

Figure 1b is similar to Fig. 1a except for $N = 48$. The magnitude of numerical accuracy in Fig. 1b should be higher than the numerical accuracy in Fig. 1a since a larger $N$ has been used. This indeed is the case for the FD4 and $\tau$ methods. Because the equal grid spacing used in the PST and SST methods is smaller than the irregular grid spacing used in the $\tau$ method at the center

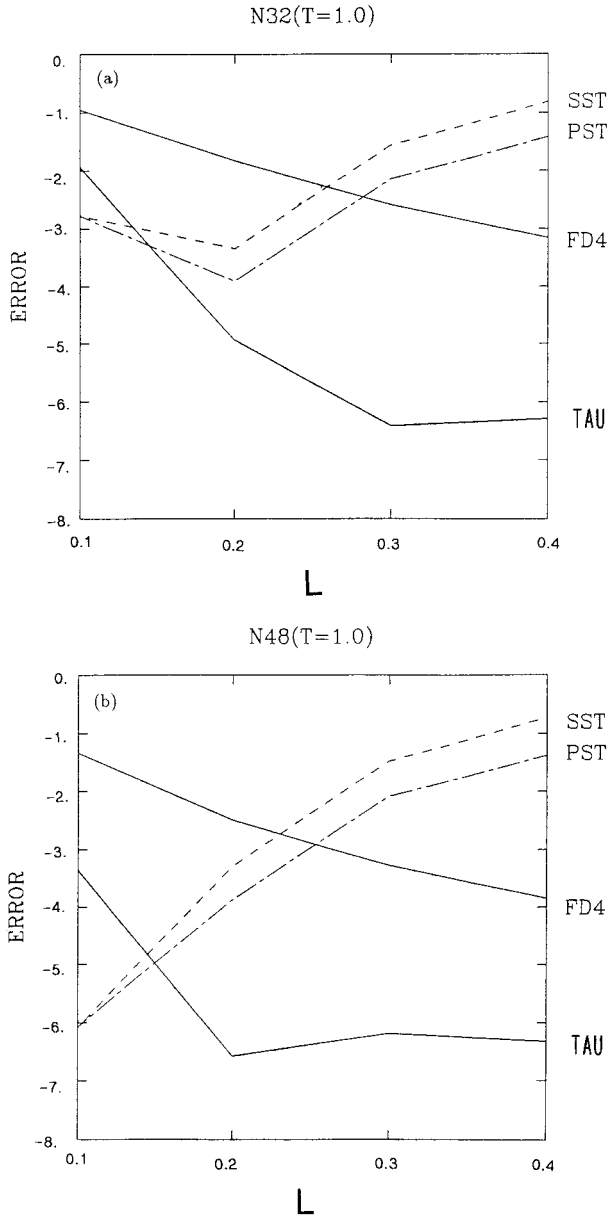


FIG. 1. Root-mean-square errors in the numerical solutions of the model problem (3.1a)–(3.1c) as a function of $L$ at $t = 1.0$ for (a) $N = 32$ and (b) $N = 48$.

of the domain, and because the discontinuity at the boundary is not felt by the smaller scale, the PST and SST methods possess the exponential convergence property and yield better results than the $\tau$ method when $L < 0.15$. We do not observe accuracy improvement from $N = 32$ to $N = 48$ in the PST and SST methods for $L \geq 0.15$. Moreover, the errors associated with the PST and SST methods increase as $L$ increases. Thus the larger spatial-scale phenomena are always modeled with less accuracy in the PST and SST methods when $N = 48$. Contrary to the Tatsumi-type method, the errors associated with the FD4 and $\tau$ methods decrease as the $L$ increases. The $\tau$ method reaches machine accuracy at $L = 0.2$. The unusual scale-dependent accuracy property we see in Fig. 1 with the PST and SST methods stems from the fact that the higher derivatives of the expanded variables in the PST and SST methods are not periodic. This discontinuity at the boundary is particularly felt by the phenomena with larger spatial scale (e.g., $L \geq 0.15$ in our model problem). Thus, large-scale phenomena are not necessarily modeled with better accuracy in the Tatsumi-type methods.

The root-mean-square errors (in log form) in numerical solutions of the model problem (3.1a)–(3.1c) as a function of $N$ and $L$ for the FD4 and $\tau$ methods at $t = 1$ are shown in Fig. 2. It is clear that the accuracy improves (until the machine accuracy of $10^{-6}$ is reached) as both $N$ and $L$ increase. Figure 3 is similar to Fig. 2 except for the PST and SST methods. Figure 3 reveals that the accuracy does not improve as $N$ increases as when $L \geq 0.2$ for both the PST and the SST methods. On the other hand, for a fixed $N$ and for $L \geq 0.2$, the accuracy is degraded as $L$ increases for both the PST and SST methods. This suggests that the discontinuity in the expanded perturbation variables not only causes the slow convergence of the sine series but also results in the unusual scale-dependent accuracy in that large spatial-scale phenomena are solved less accurately.

### *b. Poisson equation*

The root-mean-square errors in the numerical solutions of model problem (3.5) with the zero boundary condition are shown in Fig. 4 as a function of $N$ for $L = 0.2$ and $L = 0.3$. The algebraic convergence of the FD2 method for both $L = 0.2$ and $L = 0.3$ and the exponential convergence of the Fourier spectral method for $L = 0.2$ are obvious. The Fourier spectral method converges slowly for $L = 0.3$ when $N \geq 16$, and thus does not improve the accuracy as $N$ increases. This ''saturation of accuracy'' is due to the fact that the discontinuity near the boundary is felt by a larger spatial scale (e.g., $L = 0.3$) when high accuracy is desired.

Figure 5 gives the root-mean-square errors in the numerical solutions of the model problem (3.5) with the zero boundary condition as a function of the spatial-scale parameter $L$ when $N = 32$. It is clear that the errors associated with the FD2 method decrease as $L$ increases. This is the usual scale-dependent accuracy in the numerical model. Namely, the large spatial scale is resolved more accurately in the model. On the other hand, we observe the V-shaped error with respect to the size parameter $L$ for the Fourier spectral method. Again, the minimum in this V-shaped shaped curve is associated with an $L$ of 0.2. On the left part of the V-shaped curve, the error decreases more quickly than the FD2 method as $L$ increases. This reflects the exponential convergence in the Fourier spectral method over the algebraic convergence in the FD2 method. On the right part of the V-shaped curve where $L \geq 0.2$, the accuracy

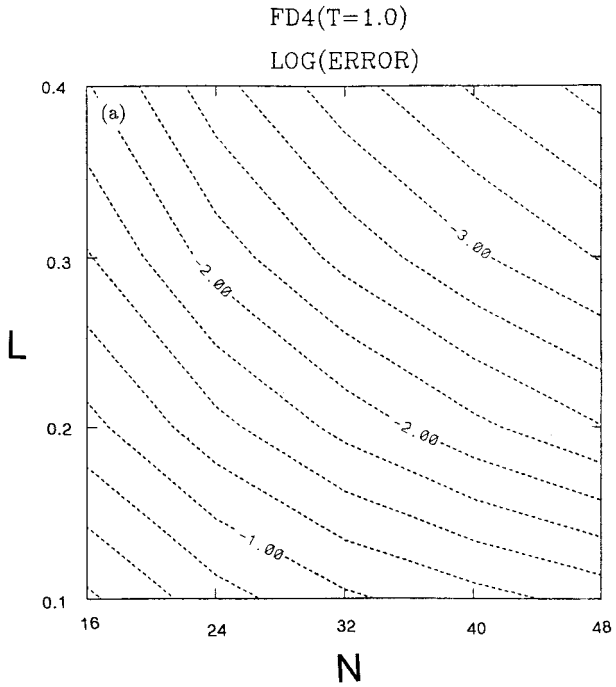


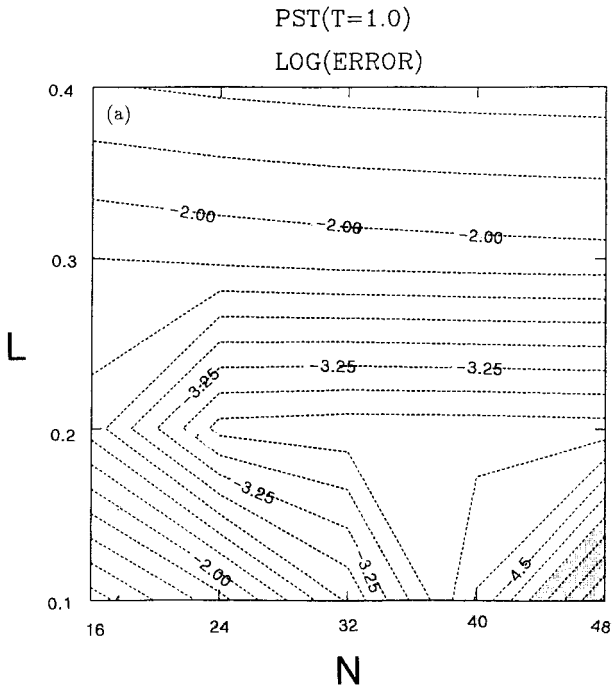


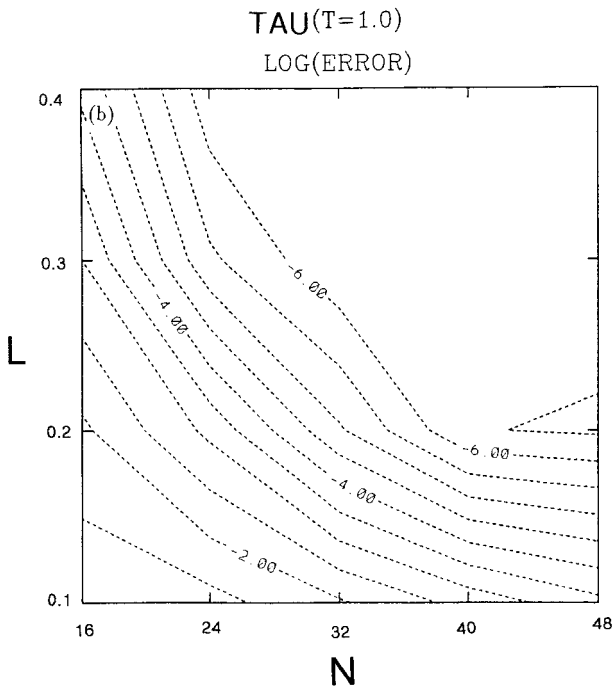


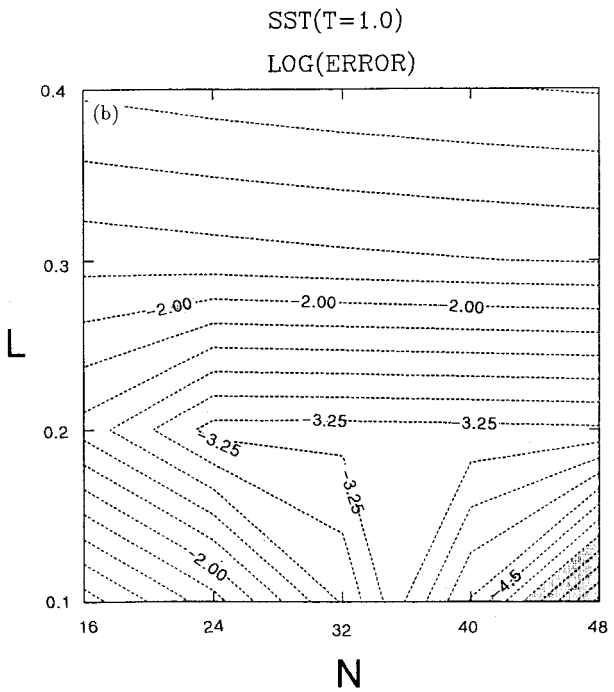


FIG. 2. Root-mean-square errors (in log form) in the numerical solutions of the model problem (3.1a)–(3.1c) as a function of $L$ and $N$ at $t = 1.0$ for (a) the FD4 method and (b) the $\tau$ method. The contour interval is 0.5.

FIG. 3. Similar to Fig. 2 except for (a) the PST method and (b) the SST method. The contour interval is 0.25.

decreases as $L$ increases. Namely, numerical accuracy associated with a larger spatial-scale phenomena is worse than the numerical accuracy associated with a smaller spatial scale. This unusual scale-dependent accuracy is accompanied with the loss of exponential convergence in the spectral model. It is also interesting to note the rapid increase of error associated with the increase of spatial-scale parameter $L$. The test of model problem (3.5) with the zero boundary condition illustrates the sensitivity of the computed solutions to the discontinuity at the boundary. This sensitivity is felt mostly for a phenomenon with larger spatial scale.

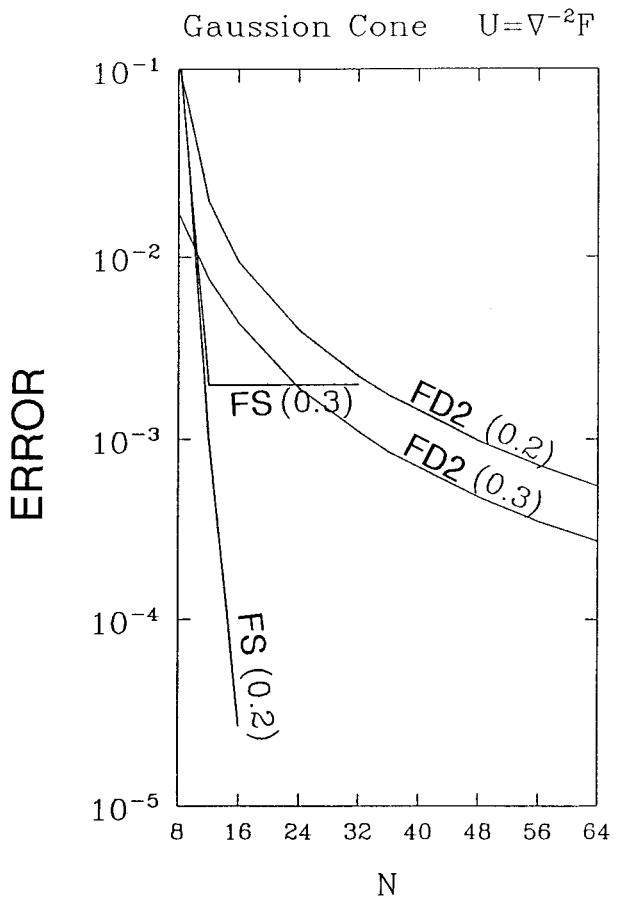


FIG. 4. Root-mean-square errors in the numerical solutions of the model problem (3.5a)–(3.5b) with the zero boundary condition as a function of $N$ for $L = 0.2$ and $L = 0.3$.

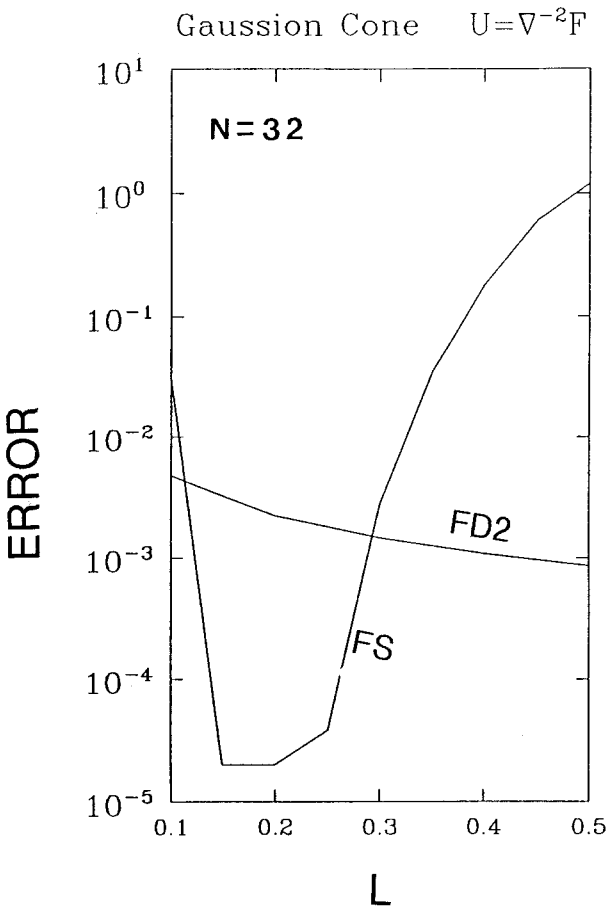


FIG. 5. Root-mean-square errors in the numerical solutions of the model problem (3.5a)–(3.5b) with the zero boundary condition as a function of $L$ when $N = 32$.

## 5. Concluding remarks

The appeal of regional spectral methods in atmospheric modeling is the accuracy and efficiency associated with the fast transform, the rapid convergence rate for the chosen basis functions, and the easy implementation of the semi-implicit method. To cope with the problem of time-dependent boundary conditions, some mean functions are often subtracted from the model variables in the Tatsumi-type methods. The subtracted model variables are then expanded in the sine–cosine basis functions to take the advantage of fast transform calculations and the easy implementation of the semi-implicit method. We have shown in this paper, by simple calculations, that the model variables expanded by sine–cosine series do not in general possess the exponential convergence property. The high-resolution solutions of regional spectral methods do not yield high accuracy accordingly. Moreover, the method possesses an unusual scale-dependent accuracy property with larger spatial-scale phenomena solved less accurately. The boundary smoothing in several regional spectral models can certainly alleviate the Gibbs phenomenon. However, the periodic condition in higher derivatives is different from the condition that the perturbation values at lateral boundaries are continuous in the higher derivatives. There are advantages in Hoyer-type methods. The buffer zone for the cyclic condition in the HIRLAM model can greatly reduce the Gibbs phenomena and thus the unusual scale-dependent accuracy associated with the model perturbation variables. Moreover, the unusual scale-dependent accuracy is associated only with the model perturbation fields in Hoyer-type methods. The model solutions in Hoyer-type spectral methods are the summation of the external components and the perturbation fields. Depending on the weighting of the perturbation fields to the total solutions in Hoyer-type spectral model, the unusual scale-dependent property may be pratically insignificant. It is not our intention to state that the unusual scale-dependent accuracy is significant in all regional models with sine–cosine series expansions.

In more complicated models, especially those intended for operational forecasting, there are sources of error besides the discretization error discussed in this

article. The errors may stem from the uncertainties in the initial conditions, from the inexact specification of boundary conditions, and from the use of physical parameterizations. Thus it is difficult, based on the calculations in this article, to assess the impact of the ''saturation of accuracy'' in the large-scale phenomena on the model output accuracy. The unusual scale-dependent accuracy in the Tatsumi-type methods may just not be important in practice. On the other hand, Lander and Hoskins (1997) try to identify the smallest resolved spatial scale that is ''believable'' for application of a sophisticated and computationally expensive parameterization scheme. They are concerned with the situation of ''garbage in, garbage out,'' in that untrustworthy fields input into a parameterization will yield an undesired feedback. The unusual scale-dependent accuracy of the regional spectral model variables, as illustrated in this paper, really complicates the argument made by Lander and Hoskins (1997) about believable scales and parameterizations in a spectral transform model. We are not in a position to state explicitly the impact of the unusual scale-dependent accuracy on an atmospheric model with sophisticated physics. This is a question for the numerical model with both the Tatsumi-type method and sophisticated physics to answer.

The Chebyshev $\tau$ method possesses exponential convergence regardless of the behavior near the boundary. The exponential convergence property of the $\tau$ method depends only on the smoothness of the model variables. No boundary smoothing or buffer zone is needed in the $\tau$ method. The exponential convergence property offers higher accuracy with fewer $N$ or greater efficiency when high accuracy is desired. However, due to the complication of solving a multidimensional elliptic equation in Chebyshev spectral space in the use of semi-implicit time integration, and due to the $O(N^{-2})$ grid spacing near the boundary in the $\tau$ method, which reduces the explicit time step significantly, it is difficult to determine which spectral method is more suitable for regional modeling. In general, the selection of numerical methods can be made only with knowledge of the particular application, including accuracy requirements and solution characteristics.

*Acknowledgments.* The authors would like to extend thanks to Professor Wayne Schubert for helpful discussions. We want to thank the reviewers for their careful review. Their comments helped to clarify our discussion with regard to the Hoyer-type spectral method. The work is supported by Grant NSC87-2111-M002-005 AP1 from the National Research Council of Taiwan. This work is partially supported by NSF Grant ATM-9525755 and P.E. 0602435N from the Office of Naval Research through the Naval Research Laboratory.

## REFERENCES

Chen, Q.-S., and Y.-H. Kuo, 1992: A harmonic-sine series expansion and its application to the partition and reconstruction problem in a limited area. *Mon. Wea. Rev.,* **120,** 91–112.

——, L.-S. Bai, and D. H. Bromwich, 1997: A harmonic spectral limited-area model with an external wind lateral boundary condition. *Mon. Wea. Rev.,* **125,** 143–167.

Fulton, S. R., and W. H. Schubert, 1987a: Chebyshev spectral methods for limited-area models. Part I: Model problem analysis. *Mon. Wea. Rev.,* **115,** 1940–1953.

——, and ——, 1987b: Chebyshev spectral methods for limited-area models. Part II: Shallow water model. *Mon. Wea. Rev.,* **115,** 1954–1965.

——, P. E. Ciesielski, and W. H. Schubert, 1986: Multigrid methods for elliptic problems: A review. *Mon. Wea. Rev.,* **114,** 943–959.

Gottlieb, D., and S. A. Orszag, 1977: *Numerical Analysis of Spectral Methods. National Science Foundation-Conference Board of Mathematical Sciences Monogr.,* No. 26, Society of Industrial and Applied Mathematics. [NTIS AD-A056922.]

Haugen, J. E., and B. Machenhauer, 1993: A spectral limited-area model formulation with time-dependent boundary conditions applied to the shallow-water equations. *Mon. Wea. Rev.,* **121,** 2618–2630.

Hoyer, J. M., 1987: The ECMWF spectral limited-area model. *Proc. ECMWF Workshop on Techniques for Horizontal Discretization in Numerical Weather Prediction Models,* Berkshire, Reading, United Kingdom, ECMWF, 343–359.

Juang, H.-M. H., and M. Kanamitsu, 1994: The NMC nested regional spectral model. *Mon. Wea. Rev.,* **122,** 3–26.

Kuo, H.-C., and W. H. Schubert, 1988: Stability of cloud-topped boundary layers. *Quart. J. Roy. Meteor. Soc.,* **114,** 887–916.

——, and R. T. Williams, 1992: Boundary effects in regional spectral models. *Mon. Wea. Rev.,* **120,** 2986–2992.

Lanczos, C., 1956: *Applied Analysis.* Prentice-Hall, 539 pp.

Lander, J., and B. J. Hoskins, 1997: Believable scales and parameterizations in a spectral transform model. *Mon. Wea. Rev.,* **125,** 292–303.

Machenhauer, B., 1986: Limited-area modeling by the HIRLAM project group. HIRLAM Tech. Rep. 1, 13pp. [Available from Danish Meteorlogical Institute, Lyngbyne; 100, 2100 Copenhagen, Denmark.]

Orszag, S. A., 1970: Transform method for calculation of vector-coupled sums: Application to the spectral form of the vorticity equation. *J. Atmos. Sci.,* **27,** 890–895.

Segami, A., K. Kurihara, H. Nakamura, M. Ueno, I. Takano, and Y. Tatsumi, 1989: Operational mesoscale weather prediction with Japan spectral model. *J. Meteor. Soc. Japan,* **67,** 907–923.

Tatsumi, Y., 1986: A spectral limited-area model with time-dependent lateral boundary conditions and its application to a multi-level primitive equation model. *J. Meteor. Soc. Japan,* **64,** 637–664.